Pediatr Radiol (2016) 46:778–790
DOI 10.1007/s00247-016-3608-9

PEDIATRIC BODY MRI

Magnetic resonance imaging of pancreaticobiliary diseases in children: from technique to practice

Sudha A. Anupindi[1] · **Nancy A. Chauvin**[1] · **Asef Khwaja**[1] · **David M. Biko**[1]

Received: 29 September 2015 / Revised: 9 February 2016 / Accepted: 11 March 2016

Abstract Magnetic resonance imaging is useful for evaluating pancreaticobiliary diseases in children after initial sonography, obviating the use of ionizing radiation or invasive procedures such as endoscopic retrograde cholangiopancreatography (ERCP) or transhepatic biliary procedures. Advanced MRI applications have improved depiction of pediatric pancreaticobiliary anatomy and have greatly impacted management of biliary and pancreatic diseases in children. In this article, we review current MRI and magnetic resonance cholangiopancreatography (MRCP) techniques and discuss their role in the assessment of common pancreatic and biliary disorders in children.

Keywords Biliary tract · Children · Magnetic resonance cholangiopancreatography · Magnetic resonance imaging · Pancreas

Introduction

Magnetic resonance imaging (MRI) and MR cholangiopancreatography (MRCP) are important noninvasive tools that obviate the use of ionizing radiation to evaluate pancreaticobiliary disorders in children. Although US is the initial modality used to evaluate pancreaticobiliary diseases, MRI provides complementary information. The addition of diffusion-weighted imaging (DWI), post-secretin imaging and selective oral and intravenous contrast agents, such as hepatocyte-specific gadolinium chelates, to standard MRCP studies can enhance the detection and depiction of pathology.

A full discussion of all pancreaticobiliary diseases is beyond the scope of this review. Here we discuss MRI techniques and then describe the role of MRI in the most common childhood conditions.

✉ Sudha A. Anupindi
anupindi@email.chop.edu

[1] Department of Radiology, The Children's Hospital of Philadelphia, University of Pennsylvania, Perelman School of Medicine, 34th Street and Civic Center Boulevard, Philadelphia, PA 19104, USA

Imaging techniques

Although US is usually the initial imaging modality performed when a pancreaticobiliary disorder is suspected in a child, additional information about anatomy and variants can be obtained from MRI/MRCP [1]. MRI and MRCP have superior soft-tissue contrast and improved visualization of ductal anatomy relative to contrast-enhanced CT [1–3]. Despite the limitations of contrast-enhanced CT, it is still valuable in the evaluation of pancreaticobiliary disease after-hours and in the emergent setting. However MRCP provides a comprehensive evaluation of the biliary and pancreatic ducts, with a heavily T2-weighted sequence allowing for visualization of the ducts at their normal physiological state. Small-caliber ducts as small as 1 mm in diameter can be seen by standard MRCP without secretin enhancement [3, 4]. Imaging is optimized at 3 tesla and using the smallest receiver coil that fits the child, along with breath-hold, respiratory gating or navigation techniques [5–7]. Additionally, sedation can be used in select populations to decrease patient motion.

Sequences

Several 2-D and 3-D sequences are acquired as part of the MRCP protocol. Conventionally, MRCP protocols comprise

coronal thick-slab T2-weighted single-shot fast spin-echo (SSFSE) and thin-section axial and coronal T2-weighted sequences with or without fat saturation. Coronal images can be obtained in any oblique plane, and thick-slab radial images provide multiple vantage points to look at the ducts (at the discretion of the radiologist). Limitations of 2-D imaging including relatively poor spatial resolution, low signal-to-noise ratio and the inability for reconstruction into other planes [6]. These issues can be overcome by obtaining a coronal 3-D T2-weighted fast spin-echo (FSE) sequence [5, 6]. Even with parallel imaging, the acquisition time for the 3-D FSE sequence can take 4–8 min (variable based on software and vendor) [5]. Therefore, either respiratory triggering or navigator gating should be applied in order to reduce motion artifact. These 3-D sequences provide higher spatial resolution, higher signal-to-noise ratio and the ability to view images on a 3-D platform to create maximum-intensity projections and other reformations. However, some authors advocate using coronal SSFSE thin and thick-slab radial imaging over 3-D T2-weighted sequences because the former are acquired in less time and have shown no significant difference in the visibility of the ducts between 2-D and 3-D images [8, 9].

Contrast agent options

Two forms of contrast agent have been employed to optimize the evaluation of pancreaticobiliary diseases: oral contrast in the form of manganese-rich juices (they make bowel lumen dark on T2-weighted sequences) and intravenous (IV) gadolinium chelates (traditional and hepatocyte-specific agents). Acai or blueberry juice can be given peroral and this nullifies the high signal contrast in the duodenum and provides better visualization of the pancreaticobiliary junction [10]. This option can potentially interfere with sedation or anesthesia protocols and should be tailored to institutional policies. Assuming no contraindications, IV gadolinium chelates are useful in evaluating pancreatic masses, necrotizing pancreatitis, abscesses and postoperative complications. Axial thin-section dynamic 3-D T1-weighted spoiled gradient echo (GRE) sequences with fat suppression in the arterial, portal-venous and delayed phases are useful to assess the pancreatic parenchyma and adjacent vascular structures. Hepatocyte-specific gadolinium agents (gadoxetate disodium) and gadobenate dimeglumine can be used in cases where delineation of the bile ducts is deemed necessary (e.g., postoperative bile leak or biliary obstruction) [6, 11].

Secretin stimulates pancreatic exocrine activity and can be given during MRCP evaluation to increase the conspicuity and diameter of the pancreatic duct. The use of secretin is controversial in pediatric imaging. Trout et al. [12] have described the effects of secretin as "suspect," whereas others have found that secretin aids in diagnosis of abnormal pancreaticobiliary duct junction as and increases the sensitivity of MRCP in diagnosing early onset idiopathic chronic pancreatitis and pancreas divisum [3]. The authors use secretin in select cases to confirm chronic pancreatitis and to indirectly assess pancreas exocrine function by qualitatively grading the amount of fluid generated in the proximal small bowel after secretin stimulation [13]. Normally post secretin, a large amount of fluid distends the entire duodenum well beyond the duodenal-jejunal junction [13]. There have been both semi-qualitative (scoring the amount of duodenal fluid [0–3] as none, minimal, adequate or normal) and objective quantitative methods (using regions of interest of the T2-bright duodenal fluid and plotting duodenal signal intensity over time) to quantify exocrine function [13, 14].

Pancreatic diseases

Pancreatitis

Pancreatitis in children can lead to substantial morbidity and mortality, primarily from associated complications. Although acute pancreatitis is reversible, chronic pancreatitis leads to irreversible destruction of the parenchyma and ducts, with loss of endocrine and exocrine function. The incidence of acute pancreatitis has been increasing over the last few decades, with an estimated 3–13 cases occurring annually per 100,000 children [15]. The list of causes of acute pancreatitis is long. However, common etiologies include idiopathic, biliary disease, trauma, structural anomalies, multisystem diseases, drugs and toxins, and infections [15]. Data on chronic pancreatitis in children are less well established [1]. The most common causes of chronic pancreatitis in children include cystic fibrosis, idiopathic, fibrosing and autoimmune pancreatitis, hereditary chronic pancreatitis and inborn errors of metabolism [15]. Hereditary pancreatitis has been linked to a trypsin mutation [6]. In acute pancreatitis, a combination of US and monitoring of constitutional symptoms and laboratory values typically suffices to guide management. However, for complicated clinical scenarios, MRI can be useful to guide management.

In acute pancreatitis, the pancreas is enlarged and swollen, with smooth effacement of the normal contour, and is hypointense on T1-weighted and hyperintense on T2-weighted sequences, with peri-pancreatic inflammation [16]. When inflammation is confined to a specific area of the pancreas, the resulting focal pancreatitis can mimic a neoplasm (Fig. 1) [16]. MRI can help elucidate specific causes of pancreatitis, such as an obstructing stone, pancreatic duct variant or other congenital anomalies (Figs. 2 and 3). However MRI should be avoided in the acute phase when edema and inflammation can obscure small duct anomalies and stones.

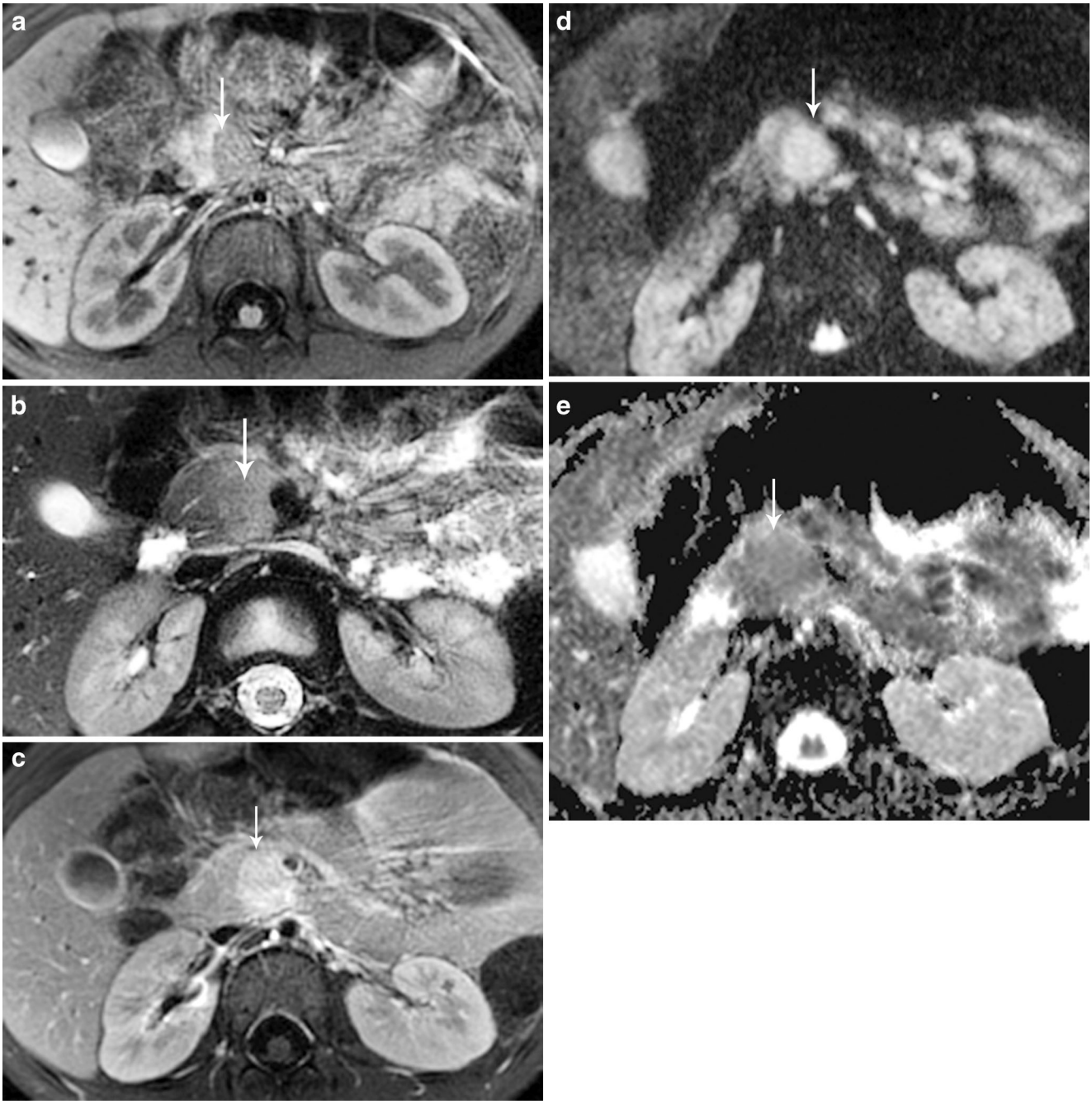

Fig. 1 MRI of a focal mass in an 8-year-old girl with elevated lipase level. Axial T1-weighted (**a**), T2-weighted (**b**) and T1-weighted post-contrast (**c**) sequences show a focal mass (*arrows*) that is hypointense on T1-weighted, hyperintense on T2-weighted and enhances homogeneously. **d** Axial diffusion-weighted image (b = 800) shows hyperintense signal within the mass (*arrow*). **e** Apparent diffusion coefficient map shows hypointense signal within the mass (*arrow*), consistent with diffusion restriction. At surgery this focal palpable hard mass was pathologically proved to be focal pancreatitis with some chronic features, although no other stigmata of chronic pancreatitis were found on MRI

Complications can be seen in both acute and chronic pancreatitis, including pseudocyst, necrosis, hemorrhage, vascular thrombosis, vascular pseudoaneurysm, abscess and, rarely, pancreaticopleural fistula [17]. Hemorrhage can be seen on MRI as an area of hyperintensity on a T1-weighted sequence (Fig. 4). Necrotizing pancreatitis is uncommon in the pediatric population and is defined as necrosis involving more than 30% of the pancreas or more than 3 cm^2 of the pancreas [18]. This is confirmed on post-contrast sequences as areas of non-enhancing parenchyma (Fig. 5). Pseudocysts are loculated fluid collections encased by a membrane of granulomatous tissue and develop greater than 4 weeks after the

Fig. 2 Acute pancreatitis and choledochal cyst in a 36-month-old girl. A coronal maximum-intensity projection created from a 3-D T2-weighted fast spin-echo MR data set demonstrates type 4a choledochal cyst (*Chc*), based on the Todani classification, compressing on the pancreas and resulting in pancreatic duct dilatation (*arrow*). There was no long common channel in this case

pancreatitis begins [15, 19]. MRCP can be used to identify communication with the pseudocyst and pancreatic duct, and post-contrast imaging can suggest superinfection if the rim of the pseudocyst is thickened and enhancing [15, 19, 20]. Careful evaluation of the vessels adjacent to the pancreas is also important because splenic vein thrombosis and splenic artery pseudoaneurysm formation can occur in severe cases.

Chronic pancreatitis

The hallmark of chronic pancreatitis on MRCP imaging is evidence of morphological change within the gland, such as pancreatic atrophy, irregular gland contours, pancreatic duct

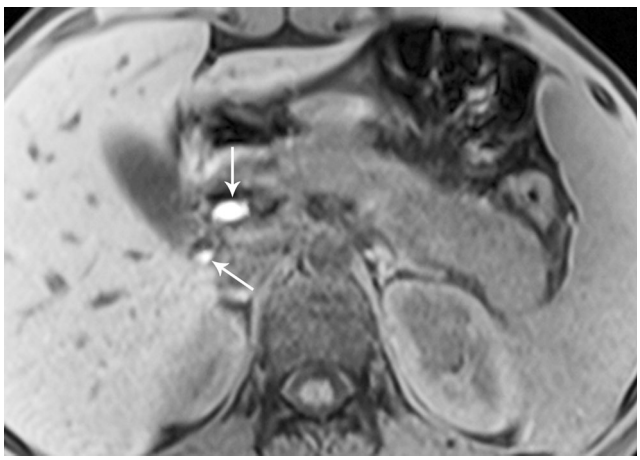

Fig. 3 MRI in a 14-year-old boy with jaundice and prior US imaging that showed gallbladder sludge. Axial T1-weighted 3-D GRE VIBE sequence shows hyperintense pigmented stones (*arrows*) in both the cystic duct and the common bile duct. This boy with choledocholithiasis went on to have endoscopic retrograde cholangiopancreatography for removal of the stones. *GRE* gradient recalled echo, *VIBE* volumetric interpolated breath-hold examination

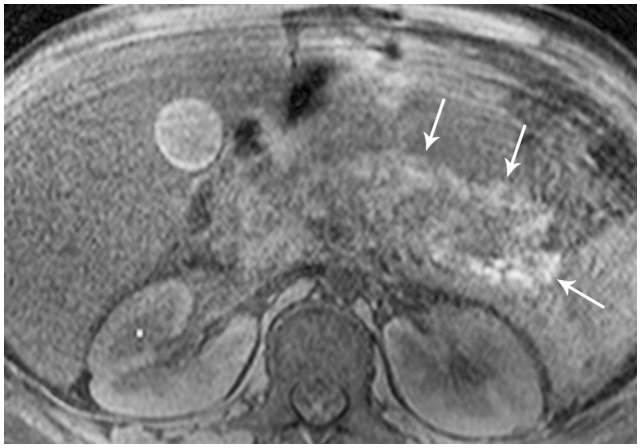

Fig. 4 Hemorrhagic pancreatitis in a 12-year-old boy with B cell acute lymphoblastic leukemia. Axial T1-weighted gradient recalled echo VIBE MR image shows hyperintensity (*arrows*) around the distal body and tail of the pancreas, which represents hemorrhage. *VIBE* volumetric interpolated breath-hold examination

dilatation, visualization of side branches, pancreatic duct strictures and parenchymal calcifications (Fig. 6) [19]. MRCP can help to determine the etiology of chronic pancreatitis, particularly congenital abnormalities.

Congenital anomalies of the pancreatic duct

Pancreas divisum

During embryological development, when the ventral and dorsal pancreatic anlages fail to fuse pancreas divisum develops. In this configuration, the majority of the gland empties into the minor papilla through the dorsal duct of Santorini, and

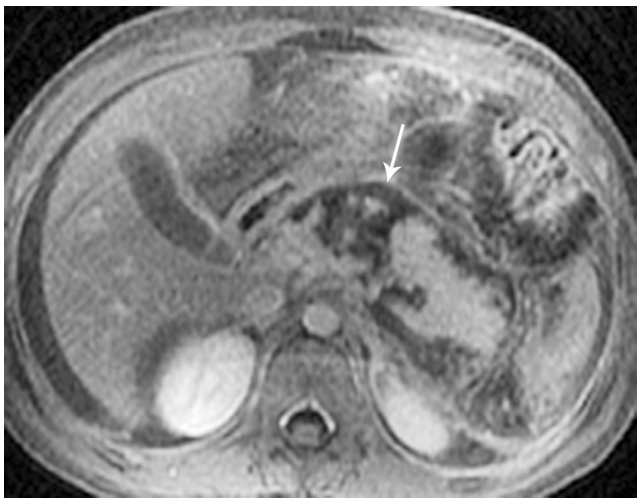

Fig. 5 Necrotizing pancreatitis in a 7-year-old boy. Axial post-contrast T1-weighted MR image shows non-enhancing area in pancreas (*arrow*), consistent with necrosis. The boy had a long course in the intensive care unit but eventually recovered

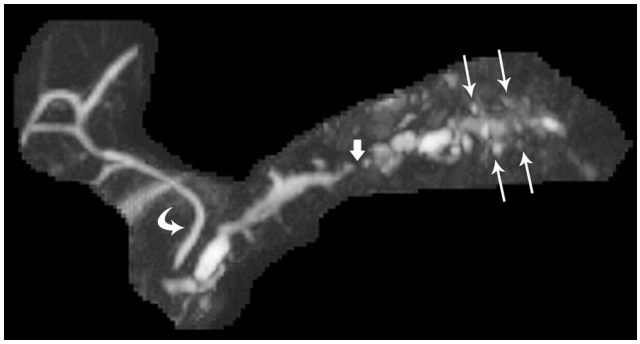

Fig. 6 Chronic pancreatitis in a 14-year-old boy with hereditary pancreatitis. This volume-rendered maximum-intensity projection reconstruction from a 3-D T2-weighted MR fast spin-echo volumetric acquisition depicts the changes of chronic pancreatitis: dilated pancreatic duct with dilated side branches (*thin arrows*) and a focal area of stricture (*thick arrow*). The common bile duct (*curved arrow*) is normal

the ventral duct of Wirsung drains only the ventral pancreatic anlage through the major papilla. The pancreatic duct and the common bile duct (CBD) drain into separate orifices, and this impaired drainage of the pancreatic duct through the minor papilla can lead to acute and chronic pancreatitis in children (Fig. 7) [6, 16]. In addition to evaluating for ductal anatomy, MRCP can be helpful to demonstrate signs of associated chronic pancreatitis [6, 16].

Fig. 7 Acute recurrent pancreatitis in a 32-month-old girl found to have pancreas divisum. A shaded surface display reconstruction from a 3-D T2-weighted fast spin-echo sequence confirms that the dorsal pancreatic duct is draining slightly cephalad toward the minor papilla (*straight arrow*), whereas the common bile duct is draining into the expected location of the major papilla (*curved arrow*)

Anomalous pancreaticobiliary junction

An anomalous pancreaticobiliary junction occurs when the junction of the pancreatic duct and CBD occurs before the ducts enter the duodenal wall. It has been reported in up to 83% of children imaged with MRCP [21]. Note that this is a single report and describes unusually high numbers, but this has not been the experience of the authors. The abnormal union has been implicated as a cause of choledochal cyst formation and pancreatitis (Fig. 8). It is hypothesized that the resultant long common

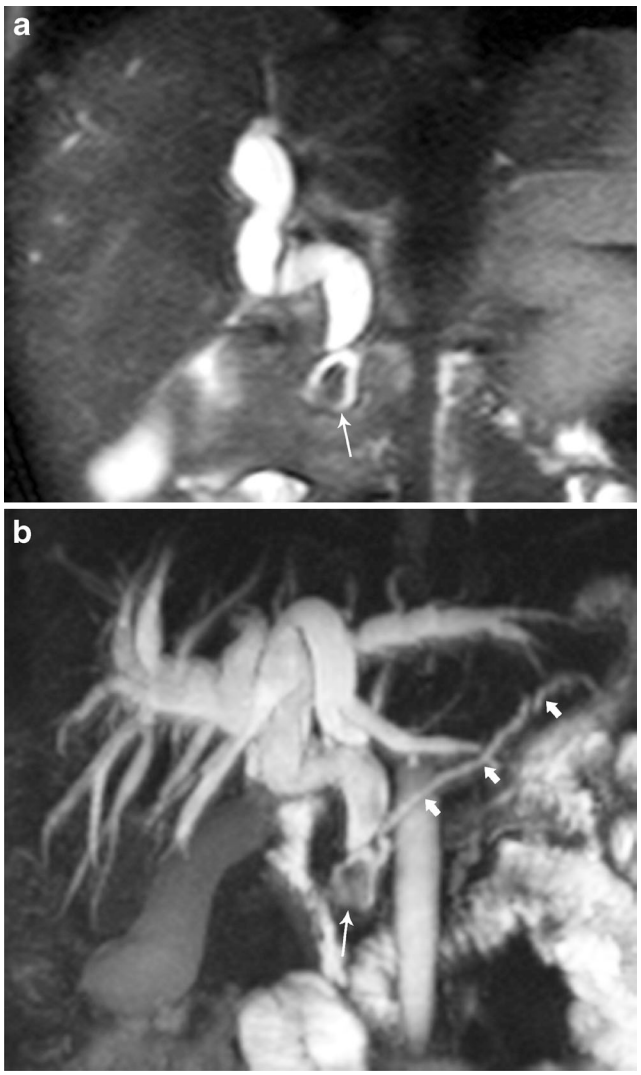

Fig. 8 Anomalous pancreaticobiliary junction in a 1-year-old girl with elevated pancreatic enzymes and US findings of biliary dilatation. **a** Coronal T2-weighted single-shot fast spin-echo (HASTE) MRI reveals fusiform dilatation of the common bile duct, with a filling defect representing a stone distal to the pancreaticobiliary junction (*arrow*). **b** Coronal T2-weighted 3-D maximum-intensity projection MRI shows a long common channel of 11 mm; the stone is lodged distal to the anomalous pancreaticobiliary junction (*thin arrow*), causing secondary pancreatitis with a dilated upstream pancreatic duct (*thick arrows*). *HASTE* half-Fourier acquisition single-shot turbo spin echo

channel is outside the sphincter of Oddi, which allows pancreatic juices and bile to freely reflux [22]. In adults, a common channel greater than 15 mm in length is considered abnormal [23]. In children there are limited data; however one pediatric publication has reported an upper limit of 5 mm [3, 6]. It can be challenging to identify an anomalous pancreaticobiliary junction, particularly in children who commonly have large choledochal cysts that obscure the underlying anatomy. In these cases secretin-MRCP can improve visualization of the long common channel [3].

Pancreatic trauma

Most pediatric pancreatic injuries are caused by blunt abdominal trauma such as bicycle handlebar injuries or motor vehicle accidents [24]. However an equally important but overlooked cause of pancreatic trauma is non-accidental trauma. The conventional method of assessing the degree of pancreatic injury has been the use of serial amylase levels along with abdominal US and contrast-enhanced CT [24]. In the evaluation of pancreatic ductal injury, CT has only demonstrated sensitivities of 43–70% in adults [25]. Although ERCP is the most sensitive method for the diagnosing pancreatic duct injury, it is invasive, exposes the child to potential complications and ionizing radiation, and is difficult to obtain in the unstable child [25].

MRCP is an emerging modality to evaluate pancreatic ductal injury in children. No study has evaluated the use of MRI for traumatic injury in the pediatric population, but several studies have demonstrated its utility in the adult population [26–30]. In a small study by Panda et al. [28], MRI accurately graded pancreatic injury in 13 of 14 adults, performing better than CT. MRI also had a sensitivity of 92% and specificity of 100% in correctly identifying pancreatic ductal injury [28]. In another study, MRCP detected not only the site of duct disruption accurately in all patients but also demonstrated additional upstream segments of ductal injury not seen on ERCP [30]. MR imaging features of acute pancreatic injury can include a complete pancreatic fracture with discontinuity in the gland (Fig. 9). If there is pancreatic ductal injury, there can be a focal disruption of the duct with proximal dilatation of the pancreatic duct. Additionally, peripancreatic fluid collections can be seen arising from the areas of the disrupted pancreatic duct (Fig. 9) [29, 30]. One more important finding in these cases is a difference in signal intensity between pancreatic parenchyma proximal and distal to the pancreatic duct injury. This is most strikingly visible on T1-weighted GRE images [26, 30]. Unfortunately, inflammation, edema and fluid in and adjacent to the pancreas can limit visualization of duct injuries. In these cases secretin-MRCP can be helpful.

Secretin MRCP has been advantageous in visualizing particularly non-dilated pancreatic ducts, and this can be useful in directing surgical therapy [29]. Secretin MRCP can depict a discrete leak from the point of pancreatic duct disruption, or increasing fluid at the point of disruption, and has been shown to aid in the management

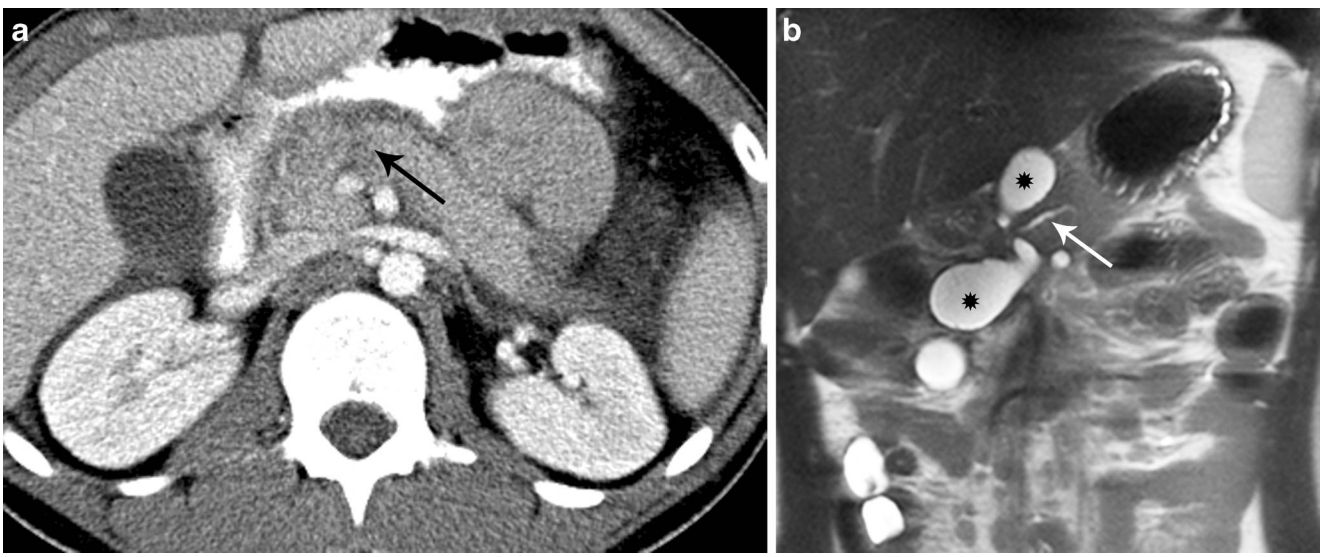

Fig. 9 Pancreatic laceration in a 16-year-old boy who presented with abdominal pain after an assault. **a** Contrast-enhanced CT examination of the abdomen shows edema within the pancreatic head, with more linear low attenuation extending through the pancreatic neck (*arrow*), consistent with a pancreatic laceration. The pancreatic duct could not be visualized. **b** Follow-up MR cholangiopancreatography 2 months later demonstrates a dumbbell-shaped pancreatic pseudocyst (*) at the site of the pancreatic laceration, which was in continuity with the pancreatic duct (*arrow*)

of adults with pancreatic injury; however there have been no dedicated pediatric studies [31].

Neoplasms of the pancreas

Pancreatic neoplasms are relatively uncommon in children and typically have a better prognosis than their counterparts in adults. Pediatric pancreatic tumors are usually well demarcated and expansile, rather than infiltrating [32]. US is commonly used to initially diagnose the mass [33]. Further evaluation is frequently performed with MRI using a combination of unenhanced and dynamic gadolinium-chelate-enhanced T1-weighted fat-suppressed sequences. In addition, on DWI solid masses sometimes show restricted diffusion [16], which might allow for earlier detection of pancreatic neoplasms as well as aid in the detection of metastases. However, the use of DWI is limited in differentiating benign from malignant pancreatic lesions because both can show restricted diffusion [34]. Pediatric pancreatic neoplasms can be divided into epithelial and non-epithelial types. Our discussion is limited to solid pseudopapillary tumors, insulinomas and lymphomas.

Solid-pseudopapillary tumor

Solid pseudopapillary tumors occur most classically in young girls. The tumors are also called solid pseudopapillary epithelial neoplasm (SPEN). These tumors are of unclear cellular origin and are considered a low-malignant-potential tumor. The pancreatic head is the most common location for solid pseudopapillary tumors in children, while the body and tail are more common in adults [32]. There is a predilection for females, blacks and East Asians. A small percentage of these tumors occurs in males [32]. Children typically present with vague abdominal pain and a mass, or they are asymptomatic and the mass is discovered on imaging for other reasons [32].

Large tumors are well-circumscribed encapsulated cystic masses containing hemorrhage or necrosis, whereas smaller tumors tend to be predominantly solid (Fig. 10) [32]. Occasionally calcifications are seen, most commonly in the capsule [32]. The hallmark of solid pseudopapillary tumors on MR is a surrounding T1- and T2-hypointense fibrous capsule with hyperintense internal T1 signal intensity consistent with hemorrhage (Fig. 10). The internal T2 signal intensity is variable because of degradation of hemoglobin. The solid portions of the tumor are iso- to hypointense to pancreas on T1-weighted imaging and iso- to slightly hyperintense to pancreas on T2-weighted imaging. After intravenous injection of a gadolinium chelate, there is slight enhancement of the solid constituents, with progressive fill-in on dynamic imaging, and the capsule also mildly enhances [32, 33]. Post-contrast images are also crucial in the evaluation of the adjacent splenic vessels and the main portal vein (Fig. 10).

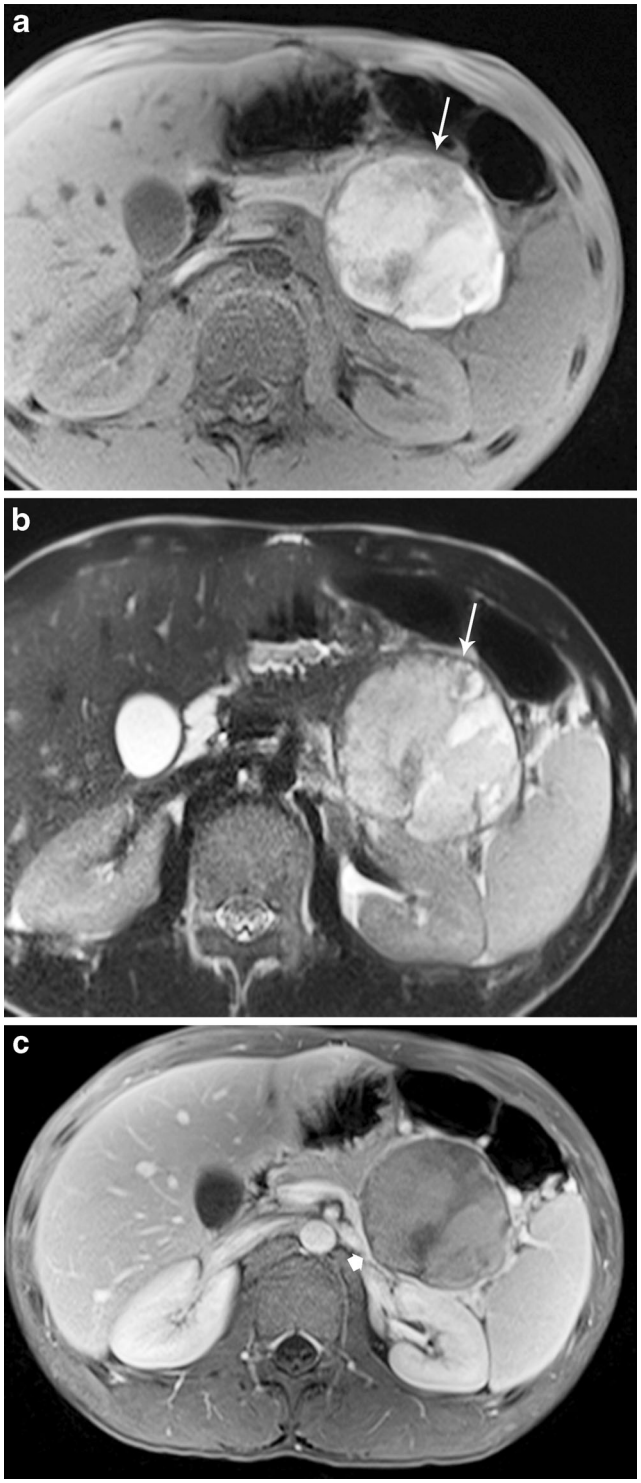

Fig. 10 Solid pseudopapillary tumor in an 11-year-old boy with 3 weeks of left upper quadrant pain and weight loss. Axial T1-weighted (**a**) and T2-weighted (**b**) MR images show a complex heterogeneous solid and cystic mass (*arrows*). High signal on the T1-weighted image is consistent with hemorrhage within the mass. **c** A delayed post-contrast fat-saturated T1-weighted MR image demonstrates only enhancement of the very thin capsule and not the internal contents of the mass. The splenic vein (*arrow*) is compressed and attenuated with mild splenomegaly. At surgery the mass was confirmed to be a solid pseudopapillary tumor and the boy required a splenectomy because of splenic congestion

Tumors of islet cell origin

Pancreatic islet cell or neuroendocrine tumors are either functional or nonfunctional. Insulinomas are the most common (functional) pancreatic neuroendocrine tumor in children [32]. While non-functional tumors present with nonspecific symptoms caused by mass effect, functional tumors are smaller and present earlier, with symptoms related to the hypersecreting hormone [32]. These lesions can be further subdivided into malignant and benign entities, with islet cell tumors accounting for 20% of malignant pancreatic tumors in children [33]. There is an increased incidence of islet cell tumors in multiple endocrine neoplasia type I and von Hippel–Lindau syndrome [32].

The role of imaging in the evaluation of a functioning islet cell tumor is not to diagnose the tumor but to localize the mass. Insulinomas are usually small (<3 cm unless malignant) and are located within the body or tail. On MR, they typically demonstrate hyperintense signal intensity on T1- and T2-weighted imaging compared to the normal pancreas; however the T2 appearance can be variable based on the amount of collagen. Homogeneous, intense gadolinium-chelate enhancement is typical in the arterial phase (Fig. 11).

Fig. 11 Functional insulinoma in a 22-year-old woman with hypoglycemia. **a** Axial T1-weighted MR image shows a hypointense focal mass in the tail of the pancreas (*arrow*). **b** Post-contrast T1-weighted image shows intense post-contrast enhancement (*arrow*). The mass was proved at surgery to be a functional insulinoma

Lymphoma

Lymphoma is the most common non-epithelial pancreatic tumor. The pancreas is involved in approximately 30% of cases of non-Hodgkin lymphoma, a finding originally described in pediatric autopsy patients, and usually involves regional, extranodal infiltration [35]. In children, pancreatic involvement is most commonly seen in large-cell lymphoma and Burkitt lymphoma [33]. Two patterns are common: a circumscribed mass or diffuse glandular enlargement mimicking acute pancreatitis [36]. Focal involvement presents as a well-defined, homogeneous T1-weighted hypointense mass with mild homogeneous enhancement (Fig. 12). The mass is usually heterogeneous and slightly

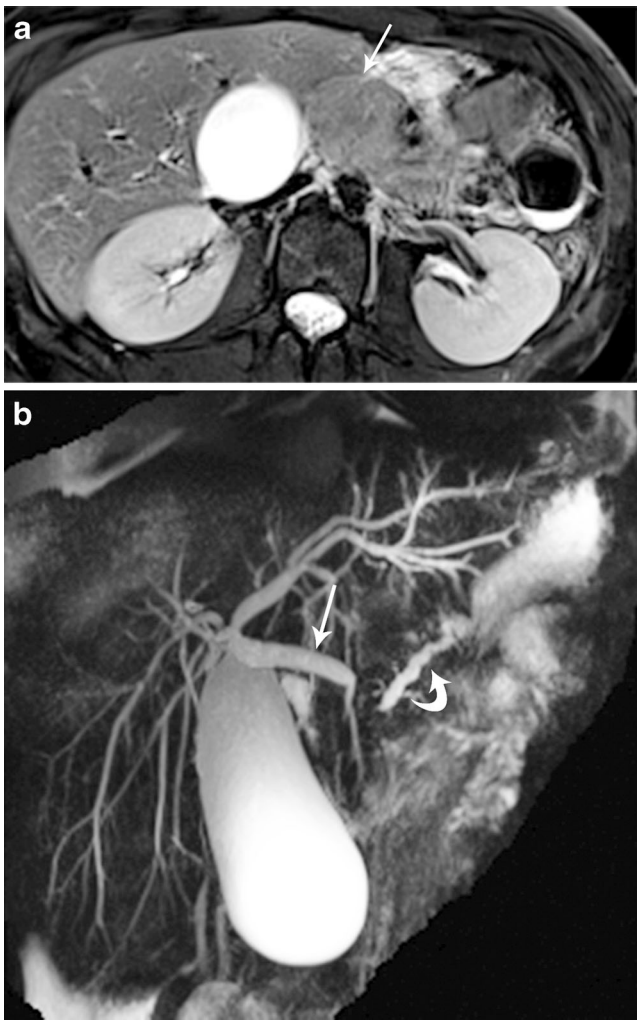

Fig. 12 Non-Hodgkin lymphoma with pancreatic involvement in a 16-year-old girl with right upper quadrant pain and jaundice. She underwent non-contrast MR cholangiopancreatography. **a** Axial high-resolution T2-weighted fat-suppressed image and (**b**) reconstructed maximum-intensity projection of the ducts show a hypointense mass in the head of the pancreas (*arrow* in **a**) resulting in dilatation of the common bile duct (*straight arrow* in **b**) and pancreatic duct (*curved arrow*) and its side branches. This was a surgically proven case of non-Hodgkin lymphoma

hyperintense on T2-weighted imaging. The diffuse variety shows enlargement of the entire pancreas, with low signal intensity on T1- and T2-weighted images and infiltration of the peri-pancreatic fat, mild to moderate enhancement, and in some cases mild pancreatic duct dilation [16].

Biliary diseases

Congenital

Congenital hepatic fibrosis is a fibropolycystic disease of the small interlobular bile ducts, whereas other fibropolycystic diseases such as Caroli disease involve large intrahepatic bile ducts [37]. Approximately 2/3 of patients with congenital hepatic fibrosis have autosomal-recessive polycystic kidney disease. Additionally, a quarter of cases of congenital hepatic fibrosis are associated with Caroli disease [38]. The clinical findings of congenital hepatic fibrosis are related to portal hypertension, predominantly splenomegaly and varices with spontaneous gastrointestinal hemorrhage [39].

MRI and MRCP are the most sensitive methods for evaluating the biliary and associated renal anomalies of congenital hepatic fibrosis [37]. Although congenital hepatic fibrosis can be present histologically even in the newborn, imaging findings might not be evident until the teenage years or even adulthood [40]. In children, the most common imaging finding is hepatosplenomegaly (Fig. 13) [41]. Additional MR imaging findings include periportal fibrosis manifested as high T2-weighted signal intensity adjacent to the portal triads, and regenerative nodules in the liver [37, 40]. On MRCP, the intrahepatic biliary ducts do not taper and remain enlarged throughout the liver parenchyma, often forming cyst-like areas (ductal ectasia) (Fig. 13) [40]. In advanced disease, there is atrophy of the right lobe of the liver with hypertrophy of the lateral segment of the left hepatic lobe and the caudate lobe, as seen in other etiologies of cirrhosis. MR angiography and venography techniques can be used to assess the hepatic vasculature, particularly in preparation for liver transplant.

Choledochal cysts

The overall incidence of choledochal cysts is 1–2 in 100,000–150,000 [42]. Choledochal cysts are much more common in the Asian population than others, with a reported prevalence of 1:1,000 in Japan [42]. People with choledochal cysts often present with cholestatic jaundice, but older children might present with abdominal pain, fever and obstructive jaundice (Fig. 14). Choledochal cysts are characterized using the Todani classification based on which biliary ducts are involved — intrahepatic, extrahepatic or both [43]. Type 1 is focal, fusiform or diffuse involvement of the CBD and common hepatic duct and accounts for 80–90% of cases [43]. Type 2 involves isolated diverticulum-like outpouching from the CBD wall [43].

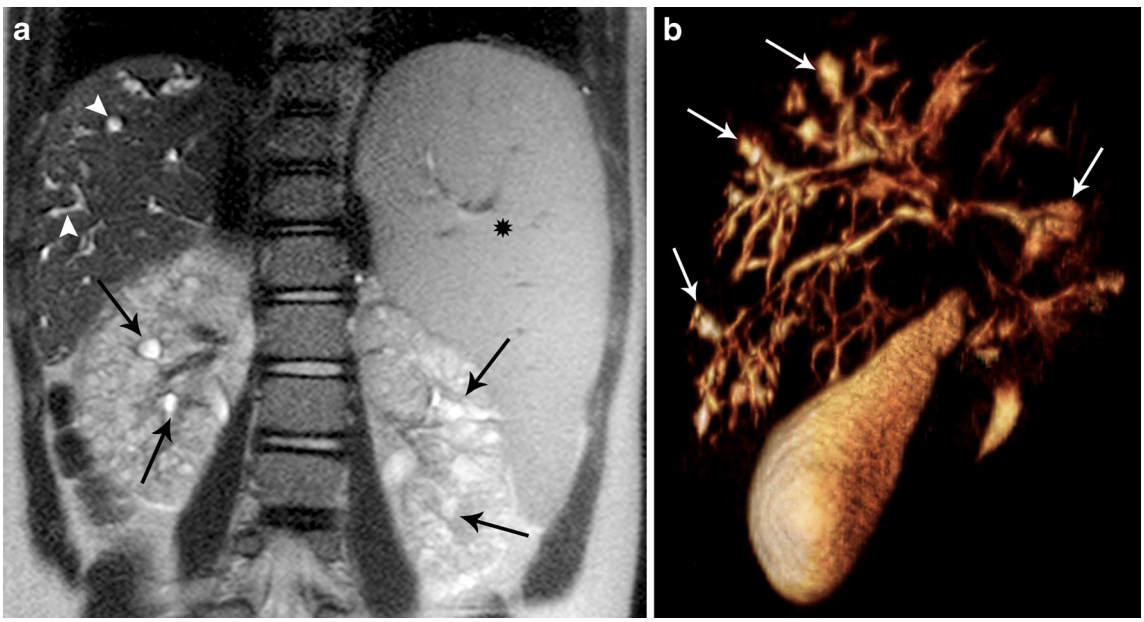

Fig. 13 Splenomegaly in a 9-year-old boy with a history of autosomal-recessive polycystic kidney disease (ARPKD) and congenital hepatic fibrosis. **a** Coronal T2-weighted image demonstrates multiple cystic lesions in both the right and left kidneys, consistent with ARPKD (*arrows*). Small cystic lesions are also noted within the liver, consistent with enlarged intrahepatic biliary ducts (*arrowheads*). Splenomegaly (*) is also noted. **b** Volume-rendered image from T2-weighted 3-D turbo spin-echo sequence shows the enlarged intrahepatic ducts (*arrows*)

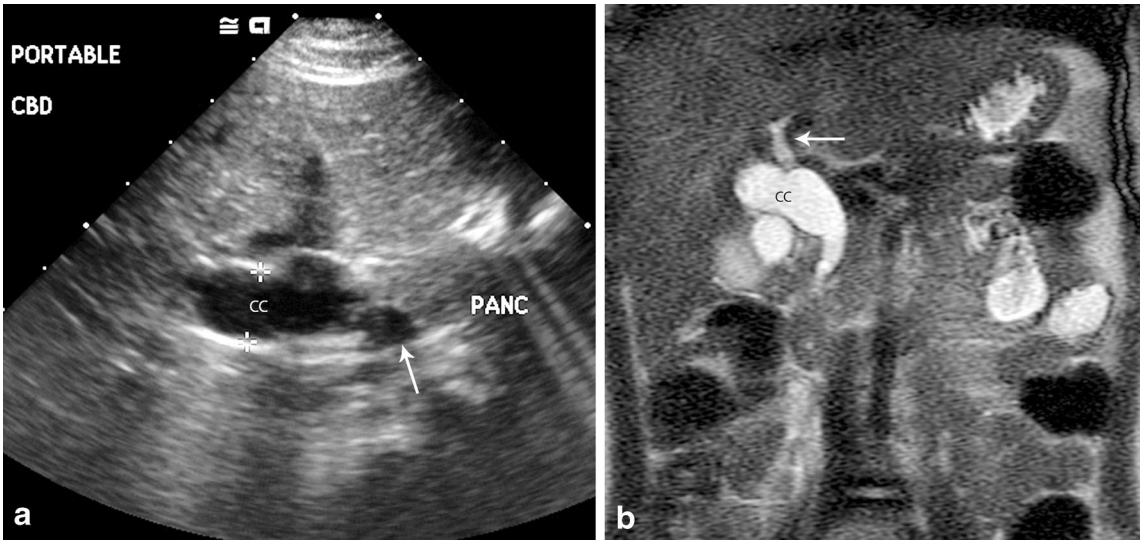

Fig. 14 Choledochal cyst in a 4-year-old girl who presented with several months of epigastric abdominal pain. **a** US image in transverse plane demonstrates a fusiform dilation of the entire common bile duct, representing the choledochal cyst (*CC*). The common bile duct is noted (*arrow*) at the head of the pancreas (*PANC*). The pancreatic duct is not dilated in this girl and could not be seen on US. **b** Coronal T2-weighted SSFSE sequence on follow-up MR cholangiopancreatography performed 1 day later better delineates the entire choledochal cyst (*CC*) and also shows the intrahepatic duct dilation on the left, from mass effect (*arrow*). *SSFSE* half-acquisition single-shot fast spin echo

Type 3 is a choledochocele, which is a cystic dilatation of the intraduodenal portion of the CBD [43]. Type 4a (Fig. 2) involves intra- and extrahepatic ducts, while type 4b consists of multiple cystic dilatations of the extrahepatic ducts alone [43]. Type 5 (Caroli disease/syndrome) involves only intrahepatic ducts [43]. US is often the initial diagnostic test in evaluation of choledochal cysts. MRCP is valuable in the preoperative workup of these patients and allows for more confident classification of the cyst and evaluation for complications, the pancreaticobiliary junction and exact measurements of size and ductal involvement. Complications of choledochal cysts include choledocholithiasis, cholangitis and, rarely, cholangiocarcinoma. MRCP has been shown to be as good as or better than conventional or endoscopic retrograde cholangiopancreatography in the evaluation of choledochal cysts, and the diagnostic accuracy of MRCP approaches 100% [3, 44].

Alagille syndrome

Alagille syndrome, also referred to as arteriohepatic dysplasia, is an autosomal-dominant hereditary disorder where there is a paucity of interlobular ducts [45]. This entity is a rare cause of neonatal cholestasis and is associated with mutations in the *JAGGED1* gene on chromosome 20 [46]. Although hepatic disease is a significant cause of morbidity in Alagille syndrome, it is not a major cause of mortality [47]. Findings of Alagille syndrome include hepatomegaly, splenomegaly, periportal fibrosis and cirrhosis. Krause et al. [48] described nodules within the liver with surrounding hypertrophic portal vessels and areas of atrophy. Large regenerative nodules along with hepatocellular carcinoma in the liver have been described in a single case report [49]. In the authors' experience (based on unpublished data and a recent publication), these regenerative nodules can be very large at presentation and can be differentiated from hepatocellular carcinoma (Fig. 15) [50]. MR imaging in Alagille syndrome is used not for diagnosis but to exclude other causes of cholestasis, follow progression of portal hypertension, and evaluate for mass development in light of underlying cirrhosis [50].

Primary sclerosing cholangitis (PSC)

Primary sclerosing cholangitis (PSC) consists of fibrosing inflammation of the intrahepatic and extrahepatic bile ducts resulting in obliteration of the bile duct lumen. PSC is increasingly recognized in children, with the incidence of 0.2 cases per year/100,000 patients [51]. PSC can be idiopathic, but it has been most commonly associated with inflammatory bowel disease, particularly ulcerative colitis [52]. In one recent study, the authors found MRCP to have a specificity and positive predictive value of 100% with an accuracy of 85%, which when correlated with the patient's clinical findings should obviate the need for ERCP [53, 54].

Characteristic MRCP findings of primary sclerosing cholangitis include the presence of multifocal strictures alternating with areas of normal or dilated ducts, giving a beaded appearance to the ducts (Fig. 16). Additionally, mild

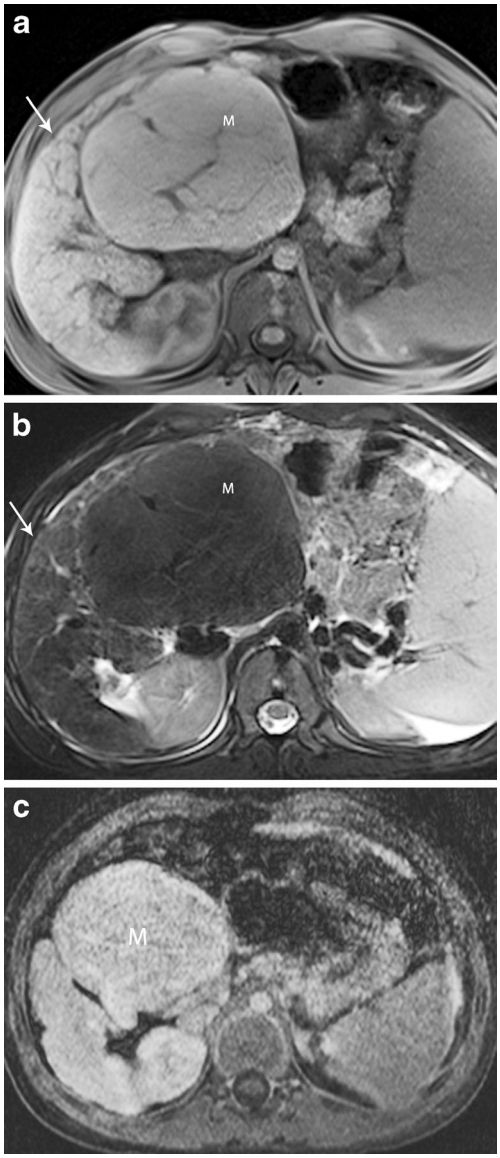

Fig. 15 Alagille syndrome in a 5-year-old girl who presented with hepatosplenomegaly and ascites, stigmata of portal hypertension. Axial T1-weighted (**a**) and axial T2-weighted (**b**) images show hepatic fibrosis and nodular liver (*arrows*), consistent with cirrhosis. There is a large well-defined mass (*M*), with large segments of the portal vein traversing through it. **c** Axial 20-min delayed post-contrast T1-weighted image with a hepatocyte-specific agent shows the mass (*M*) enhancing similarly to the adjacent liver. Biopsy confirmed a giant benign regenerative nodule without malignancy

irregularity of the duct wall, dilatation, non-visualization of intrahepatic ducts and the formation of sacculations and pseudodiverticuli in the extrahepatic ducts are sometimes seen (Fig. 16) [55].

Neoplasms of bile duct origin

Hepatobiliary rhabdomyosarcoma represents 1% of liver tumors in children, with most cases diagnosed in children younger than 5 years. Jaundice is the most common presenting symptom, with elevation of conjugated bilirubin and alkaline phosphatase and with a normal serum alpha-fetoprotein [56, 57]. MR imaging demonstrates a T1-weighted hypointense and T2-weighted hyperintense mass within the common bile duct or biliary radicals. Less commonly there is a heterogeneous intrahepatic mass with large fluid-intensity regions. Heterogeneous, intense enhancement has been described [58]. MRCP can be useful to evaluate the extent of biliary duct involvement. Evaluation should include possible adjacent organ involvement, vascular thrombosis and regional lymphadenopathy (Fig. 17) [56]. Cholangiocarcinoma is rare in children but should be considered in those with long-standing PSC.

Fig. 16 Recently diagnosed primary sclerosing cholangitis (PSC) in a 16-year-old boy who presented with scleral icterus and abdominal pain. Coronal oblique T2-weighted maximum-intensity projection reconstructed from a 3-D MR data set shows alternating strictures and dilatations (*arrows*), giving a beaded pattern of the intrahepatic ducts, as well as some areas of saccular configuration representing pseudodiverticuli involving the right hepatic ducts (*circle*)

Conclusion

In this brief review we have described MRI techniques and practical applications in assessing common pediatric

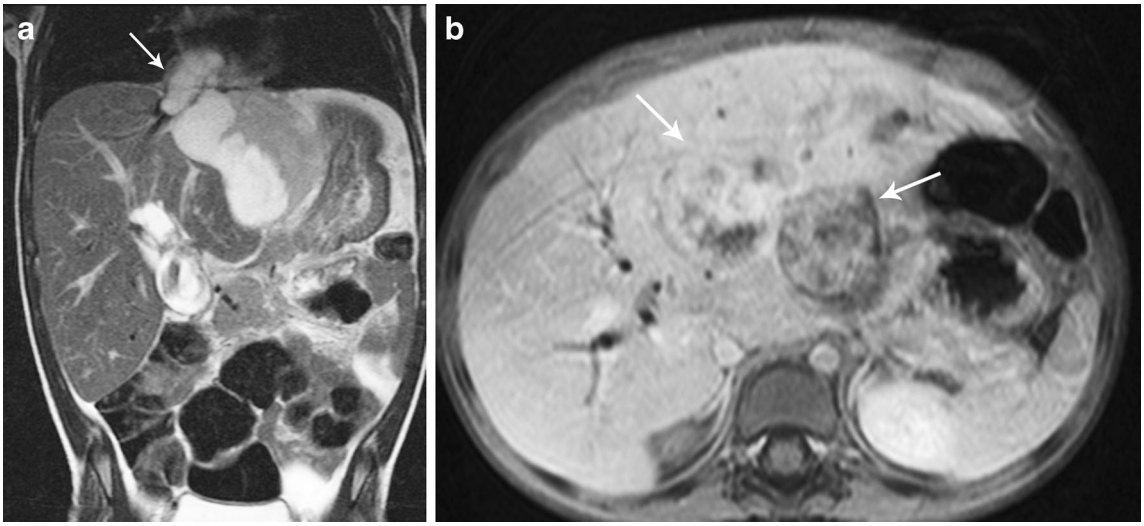

Fig. 17 Biliary rhabdomyosarcoma in a 3-year-old girl who presented with increasingly difficult breathing, fatigue and hepatomegaly. **a** Coronal T2-weighted SSFSE (HASTE) image demonstrates a predominantly intrahepatic hyperintense mass extending into the right atrium (*arrow*). **b** Axial T1-weighted post-contrast MR image shows minimal heterogeneous enhancement of the mass (*arrows*), with adjacent biliary ductal dilatation. This mass was biopsy proven biliary rhabdomyosarcoma. *HASTE* half-Fourier acquisition single-shot turbo spin-echo, *SSFSE* half-acquisition single-shot fast spin echo

pancreaticobiliary disorders. Imaging optimization allows for evaluation of the possible etiology of a process, can assess for complications and serves as a noninvasive guide for surgical and endoscopic therapies.

Compliance with ethical standards

Conflicts of interest The authors have no financial interests, investigational or off-label uses to disclose.

References

1. Darge K, Anupindi S (2009) Pancreatitis and the role of US, MRCP and ERCP. Pediatr Radiol 39:S153–S157
2. Arvanitakis M, Delhaye M, De Maertelaere V et al (2004) Computed tomography and magnetic resonance imaging in the assessment of acute pancreatitis. Gastroenterology 126:715–723
3. Chavhan GB, Babyn PS, Manson D et al (2008) Pediatric MR cholangiopancreatography: principles, technique, and clinical applications. Radiographics 28:1951–1962
4. Gwal K, Bedoya MA, Patel N et al (2015) Reference values of MRI measurements of the common bile duct and pancreatic duct in children. Pediatr Radiol 45:1153–1159
5. Costello JR, Kalb B, Chundru S et al (2014) MR imaging of benign and malignant biliary conditions. Magn Reson Imaging Clin N Am 22:467–488
6. Egbert ND, Bloom DA, Dillman JR (2013) Magnetic resonance imaging of the pediatric pancreaticobiliary system. Magn Reson Imaging Clin N Am 21:681–696
7. Almehdar A, Chavhan GB (2013) MR cholangiopancreatography at 3.0 T in children: diagnostic quality and ability in assessment of common paediatric pancreatobiliary pathology. Br J Radiol 86: 20130036
8. Chavhan GB, Almehdar A, Moineddin R et al (2013) Comparison of respiratory-triggered 3-D fast spin-echo and single-shot fast spin-echo radial slab MR cholangiopancreatography images in children. Pediatr Radiol 43:1086–1092
9. Lavdas E, Vlychou M, Arikidis N et al (2013) How reliable is MRCP with an SS-FSE sequence at 3.0 T: comparison between SS-FSE BH and 3D-FSE BH ASSET sequences. Clin Imaging 37:697–703
10. Bittman ME, Callahan MJ (2014) The effective use of acai juice, blueberry juice and pineapple juice as negative contrast agents for magnetic resonance cholangiopancreatography in children. Pediatr Radiol 44:883–887
11. Chavhan GB, Babyn PS, Temple M et al (2013) Diagnosis of postoperative bile leak and accurate localization of the site of leak by gadobenate dimeglumine-enhanced MR cholangiography in a child. Pediatr Radiol 43:763–766
12. Trout AT, Podberesky DJ, Serai SD et al (2013) Does secretin add value in pediatric magnetic resonance cholangiopancreatography? Pediatr Radiol 43:479–486
13. Sandrasegaran K, Lin C, Akisik FM et al (2010) State-of-the-art pancreatic MRI. AJR Am J Roentgenol 195:42–53
14. Sanyal R, Stevens T, Novak E et al (2012) Secretin-enhanced MRCP: review of technique and application with proposal for quantification of exocrine function. AJR Am J Roentgenol 198: 124–132
15. Srinath AI, Lowe ME (2013) Pediatric pancreatitis. Pediatr Rev 34: 79–90
16. O'Neill E, Hammond N, Miller FH (2014) MR imaging of the pancreas. Radiol Clin N Am 52:757–777
17. Nydegger A, Couper RT, Oliver MR (2006) Childhood pancreatitis. J Gastroenterol Hepatol 21:499–509
18. Banks PA, Freeman ML (2006) Practice guidelines in acute pancreatitis. Am J Gastroenterol 101:2379–2400
19. Thai TC, Riherd DM, Rust KR (2013) MRI manifestations of pancreatic disease, especially pancreatitis, in the pediatric population. AJR Am J Roentgenol 201:W877–W892
20. Hwang JY, Yoon HK, Kim KM (2015) Characteristics of pediatric pancreatitis on magnetic resonance cholangiopancreatography. Pediatr Gastroenterol Hepatol Nutr 18:73–84
21. Suzuki M, Shimizu T, Kudo T et al (2006) Usefulness of nonbreathhold 1-shot magnetic resonance cholangiopancreatography for the

evaluation of choledochal cyst in children. J Pediatr Gastroenterol Nutr 42:539–544
22. Alexander LF (2012) Congenital pancreatic anomalies, variants, and conditions. Radiol Clin N Am 50:487–498
23. Mortele KJ, Rocha TC, Streeter JL et al (2006) Multimodality imaging of pancreatic and biliary congenital anomalies. Radiographics 26:715–731
24. Stringer MD (2005) Pancreatitis and pancreatic trauma. Semin Pediatr Surg 14:239–246
25. Potoka DA, Gaines BA, Leppaniemi A et al (2015) Management of blunt pancreatic trauma: what's new? Eur J Trauma Emerg Surg 41: 239–250
26. Fulcher AS, Turner MA, Yelon JA et al (2000) Magnetic resonance cholangiopancreatography (MRCP) in the assessment of pancreatic duct trauma and its sequelae: preliminary findings. J Trauma 48: 1001–1007
27. Nirula R, Velmahos GC, Demetriades D (1999) Magnetic resonance cholangiopancreatography in pancreatic trauma: a new diagnostic modality? J Trauma 47:585–587
28. Panda A, Kumar A, Gamanagatti S et al (2015) Evaluation of diagnostic utility of multidetector computed tomography and magnetic resonance imaging in blunt pancreatic trauma: a prospective study. Acta Radiol 56:387–396
29. Ragozzino A, Manfredi R, Scaglione M et al (2003) The use of MRCP in the detection of pancreatic injuries after blunt trauma. Emerg Radiol 10:14–18
30. Soto JA, Alvarez O, Munera F et al (2001) Traumatic disruption of the pancreatic duct: diagnosis with MR pancreatography. AJR Am J Roentgenol 176:175–178
31. Gillams AR, Kurzawinski T, Lees WR (2006) Diagnosis of duct disruption and assessment of pancreatic leak with dynamic secretin-stimulated MR cholangiopancreatography. AJR Am J Roentgenol 186:499–506
32. Chung EM, Travis MD, Conran RM (2006) Pancreatic tumors in children: radiologic-pathologic correlation. Radiographics 26: 1211–1238
33. Shet NS, Cole BL, Iyer RS (2014) Imaging of pediatric pancreatic neoplasms with radiologic-histopathologic correlation. AJR Am J Roentgenol 202:1337–1348
34. Wang Y, Miller FH, Chen ZE et al (2011) Diffusion-weighted MR imaging of solid and cystic lesions of the pancreas. Radiographics 31:E47–E64
35. Ng YY, Healy JC, Vincent JM et al (1994) The radiology of non-Hodgkin's lymphoma in childhood: a review of 80 cases. Clin Radiol 49:594–600
36. Lee WK, Lau EW, Duddalwar VA et al (2008) Abdominal manifestations of extranodal lymphoma: spectrum of imaging findings. AJR Am J Roentgenol 191:198–206
37. Akhan O, Karaosmanoglu AD, Ergen B (2007) Imaging findings in congenital hepatic fibrosis. Eur J Radiol 61:18–24
38. Khanna R, Sarin SK (2014) Non-cirrhotic portal hypertension — diagnosis and management. J Hepatol 60:421–441
39. Brancatelli G, Federle MP, Vilgrain V et al (2005) Fibropolycystic liver disease: CT and MR imaging findings. Radiographics 25:659–670
40. Turkbey B, Ocak I, Daryanani K et al (2009) Autosomal recessive polycystic kidney disease and congenital hepatic fibrosis (ARPKD/CHF). Pediatr Radiol 39:100–111
41. Jung G, Benz-Bohm G, Kugel H et al (1999) MR cholangiography in children with autosomal recessive polycystic kidney disease. Pediatr Radiol 29:463–466
42. Stringer MD, Dhawan A, Davenport M et al (1995) Choledochal cysts: lessons from a 20 year experience. Arch Dis Child 73:528–531
43. Todani T, Watanabe Y, Narusue M et al (1977) Congenital bile duct cysts: classification, operative procedures, and review of thirty-seven cases including cancer arising from choledochal cyst. Am J Surg 134:263–269
44. Nievelstein RA, Robben SG, Blickman JG (2011) Hepatobiliary and pancreatic imaging in children — techniques and an overview of non-neoplastic disease entities. Pediatr Radiol 41:55–75
45. Alagille D, Estrada A, Hadchouel M et al (1987) Syndromic paucity of interlobular bile ducts (Alagille syndrome or arteriohepatic dysplasia): review of 80 cases. J Pediatr 110:195–200
46. Oda T, Elkahloun AG, Pike BL et al (1997) Mutations in the human Jagged1 gene are responsible for Alagille syndrome. Nat Genet 16: 235–242
47. Emerick KM, Rand EB, Goldmuntz E et al (1999) Features of Alagille syndrome in 92 patients: frequency and relation to prognosis. Hepatology 29:822–829
48. Krause D, Cercueil JP, Dranssart M et al (2002) MRI for evaluating congenital bile duct abnormalities. J Comput Assist Tomogr 26: 541–552
49. Wetli SC, Gralla ES, Schibli S et al (2010) Hepatocellular carcinoma and regenerating nodule in a 3-year-old child with Alagille syndrome. Pediatr Radiol 40:1696–1698
50. Alhammad A, Kamath BM, Chami R et al (2016) Solitary hepatic nodule adjacent to the right portal vein: a common finding of Alagille syndrome? J Pediatr Gastroenterol Nutr 62:226–232
51. Kaplan GG, Laupland KB, Butzner D et al (2007) The burden of large and small duct primary sclerosing cholangitis in adults and children: a population-based analysis. Am J Gastroenterol 102: 1042–1049
52. Wilschanski M, Chait P, Wade JA et al (1995) Primary sclerosing cholangitis in 32 children: clinical, laboratory, and radiographic features, with survival analysis. Hepatology 22: 1415–1422
53. Ferrara C, Valeri G, Salvolini L et al (2002) Magnetic resonance cholangiopancreatography in primary sclerosing cholangitis in children. Pediatr Radiol 32:413–417
54. Chavhan GB, Roberts E, Moineddin R et al (2008) Primary sclerosing cholangitis in children: utility of magnetic resonance cholangiopancreatography. Pediatr Radiol 38:868–873
55. Vitellas KM, Keogan MT, Freed KS et al (2000) Radiologic manifestations of sclerosing cholangitis with emphasis on MR cholangiopancreatography. Radiographics 20:959–975
56. Chung EM, Lattin GE Jr, Cube R et al (2011) From the archives of the AFIP: pediatric liver masses: radiologic-pathologic correlation. Part 2. Malignant tumors. Radiographics 31:483–507
57. Donnelly LF, Bisset GS 3rd, Frush DP (1998) Diagnosis please. Case 2: embryonal rhabdomyosarcoma of the biliary tree. Radiology 208:621–623
58. Roebuck DJ, Yang WT, Lam WW et al (1998) Hepatobiliary rhabdomyosarcoma in children: diagnostic radiology. Pediatr Radiol 28: 101–108